https://doi.org/10.5194/egusphere-2026-4216
Preprint. Discussion started: 28 July 2026

A multi-site climatology of aerosol mixing state from hygroscopicity measurements

Yicen Liu[a], Shengqian Zhou[b], Jian Wang[b], and Nicole Riemer[c]

[a]Department of Civil and Environmental Engineering, Grainger College of Engineering, University of Illinois Urbana-Champaign, Urbana, IL, USA
[b]Department of Energy, Environmental, and Chemical Engineering, Washington University in St. Louis, St. Louis, MO, USA
[c]Department of Climate, Meteorology, and Atmospheric Science, University of Illinois Urbana-Champaign, Urbana, IL, USA

Correspondence: Nicole Riemer (nriemer@illinois.edu)

Abstract. We present an expanded, size-resolved observational climatology of aerosol mixing state inferred from hygroscopicity measurements. Using κ-PDFs from long-term and campaign-based HTDMA observations at eight sites spanning urban, continental, coastal, marine environments, we infer the aerosol mixing state index χ across multiple particle sizes and four seasons. Building on a previously evaluated κ-to-χ framework, we synthesize these datasets to characterize spatial, seasonal, and size-dependent variability in aerosol mixing state, with attention to retrieval limitations and site-dependent. We find that continental and accumulation-mode aerosol populations generally exhibit consistently higher χ, whereas marine and urban-influenced sites tend to be more externally mixed and show greater variability. Across most sites, χ increases with particle size, consistent with the stronger atmospheric aging of accumulation-mode particles. The use of D_α–D_γ diagnostics provides insight into the processes controlling the observed variability in χ. These results provide observational constraints on the size dependence, seasonal variability, and environmental controls of aerosol mixing state, and establish benchmarks for evaluating mixing-state assumptions in aerosol models relevant to cloud activation and radiative effects.

1 Introduction

Atmospheric aerosol particles are complex mixtures consisting of diverse chemical species distributed in varying proportions across individual particles within a population (Bondy et al., 2018). This particle-to-particle variability in chemical composition is captured by the concept of aerosol mixing state, which describes how chemical species are distributed among individual particles rather than simply characterizing bulk composition (Riemer and West, 2013). At one extreme, a fully internally mixed population has all particle sharing the same composition as the bulk; at the other extreme, a fully externally mixed population consists of particles each composed of a single pure chemical species. Real atmospheric aerosols fall between these two extremes, and their mixing state evolves continuously through emission, coagulation, condensation, chemical aging, and cloud processing (Ebert et al., 2004; Moffet et al., 2010; Laskin et al., 2012; Zaveri et al., 2012; Adachi et al., 2022).

Aerosol mixing state has important consequences for aerosol-cloud and aerosol-radiation interactions, as it affects cloud condensation nuclei activity (Cubison et al., 2008; Wang et al., 2010; Leck and Svensson, 2015), light scattering and absorption (Zhao et al., 2021a; Yao et al., 2022; Zeng et al., 2024), and heterogeneous chemistry in ways that bulk composition

https://doi.org/10.5194/egusphere-2026-4216
Preprint. Discussion started: 28 July 2026

alone cannot capture (Baustian et al., 2012; Liu et al., 2025b). Despite its importance, aerosol mixing state remains one of the least constrained properties in regional and global aerosol models. Most current earth system models represent aerosol populations using modal or sectional approaches, in which particles within a given mode or size bin are assumed to be internally mixed. Some models adopt the opposite extreme, representing particle populations as fully externally mixed, with each mode containing particles of a single chemical type such that sulfate, black carbon, and organic carbon reside in separate particle populations (Kleeman and Cass, 2001; Chin et al., 2002). The simplified aerosol representations have been shown to introduce systematic biases in predicted aerosol optical properties, CCN concentrations, and radiative forcing estimates (Zhu et al., 2016; Zheng et al., 2021; Yao et al., 2022). Bridging the gap between model assumptions and atmospheric reality therefore requires long-term, cross-site, size-resolved observational constratins that allow comparison across environments and seasons.

Current observational constraints on aerosol mixing state remain insufficient to meet this requirement. Direct characterization of per-particle composition, through techniques such as single-particle mass spectrometry, electron microscopy, or X-ray spectroscopy, has demonstrated that mixing state varies substantially across environments and particle sizes (Fraund et al., 2017; Lata et al., 2021; Xue et al., 2024; Wu et al., 2024). However, these measurements are inherently campaign-specific and short in duration, rarely coordinated across multiple sites to allow systematic spatial or seasonal comparisons. Establishing a climatological perspective on aerosol mixing state variability is therefore essential to provide the observational foundation needed to evaluate and improve mixing state representations in atmospheric models.

Hygroscopicity measurements offer a practical pathway toward addressing this limitation. The Hygroscopic Tandem Differential Mobility Analyzer (HTDMA) provides size-resolved probability distributions of the hygroscopicity parameter κ (κ-PDFs) that reflect particle-to-particle composition variability at each selected diameter. HTDMA instruments operate continuously and are deployed at long-term monitoring networks and field campaigns worldwide, providing datasets that span multiple years and diverse environments. Yuan and Zhao (2023) proposed an elegant method to translate κ-PDFs into the mixing state index (χ) by assuming individual aerosol particles as binary mixtures of more-hygroscopic (MH) and less-hygroscopic (LH) components. Liu et al. (2026) systematically evaluated this retrieval using particle-resolved simulations, demonstrating its reliability across a wide range of continental aerosol conditions.

Here we build on the evaluated retrieval framework to present an expanded, size-resolved observational climatology of aerosol mixing state derived from long-term hygroscopicity measurements. We apply the method of Yuan and Zhao (2023) to HTDMA datasets from eight sites spanning urban, continental, coastal, and marine environments, across multiple particle sizes and seasons. From these retrievals, we characterize the spatial, size-dependent, and seasonal variability of aerosol mixing state across diverse atmospheric environments. We further examine the retrievals in D_α–D_γ space to assess how changes in average particle-level diversity and bulk population diversity contribute to the observed variability in χ. The resulting climatology provides practical observational benchmarks for evaluating mixing-state representations in atmospheric models.

The paper is structured as follows: Section 2 briefly revisits the hygroscopicity-based mixing state retrieval framework. Section 3 describes the HTDMA datasets and site characteristics. Section 4 presents the κ-based χ climatology.

https://doi.org/10.5194/egusphere-2026-4216
Preprint. Discussion started: 28 July 2026

2 Hygroscopicity-based aerosol mixing state retrieval

The aerosol mixing state index χ quantifies the degree of internal versus external mixing within an aerosol population, ranging from 0% for a fully externally mixed population to 100% for a fully internally mixed population (Riemer and West, 2013). We infer χ from the HTDMA-measured κ-PDF using the framework of Yuan and Zhao (2023). In this framework, each particle is represented as a binary mixture of less hygroscopic (LH) and more hygroscopic (MH) components. Their volume fractions in the i^{th} κ-bin are expressed as:

$$P_{i,\mathrm{MH}} = \frac{\kappa_i - \kappa_{\mathrm{LH}}}{\kappa_{\mathrm{MH}} - \kappa_{\mathrm{LH}}}, \tag{1}$$

$$P_{i,\mathrm{LH}} = 1 - P_{i,\mathrm{MH}}, \tag{2}$$

where κ_i is the hygroscopicity parameter κ at bin i, κ_{LH} and κ_{MH} are prescribed end-member hygroscopicities.

For continental and coastal sites, we follow Liu et al. (2026) and prescribe $\kappa_{\mathrm{LH}} = 0$ for the nearly non-hygroscopic carbonaceous end-member and $\kappa_{\mathrm{MH}} = 0.65$ for the more hygroscopic inorganic end-member, representing aerosol dominated by sulfate, nitrate, and ammonium. For the marine-influenced sites ENA (Eastern North Atlantic) and MHD (Mace Head, Ireland), we instead use $\kappa_{\mathrm{MH}} = 1.5$ to encompass the highly hygroscopic tail associated with marine aerosol, such as sea salt, sulfuric acid, and ammonium bisulfate. This broader end-member range makes the binary representation more approximate because common inorganic particles may be interpreted as LH/MH mixtures rather than pure MH material, potentially biasing the retrieved χ high. The values obtained at ENA and MHD should therefore be regarded as first-order estimates of temporal and size-dependent variability and are not directly comparable with values retrieved using $\kappa_{\mathrm{MH}} = 0.65$.

The equations above assign an LH/MH composition to the particles in each κ bin, while the κ-PDF specifies the relative abundance of particles in that bin. These quantities are used to calculate the average particle-level diversity D_α, and the population-level bulk diversity D_γ. The mixing state index is then calculated as:

$$\chi = \frac{D_\alpha - 1}{D_\gamma - 1}. \tag{3}$$

Details of the derivation, sensitivity analysis, and uncertainty evaluation are provided by Liu et al. (2026).

3 Long-term HTDMA Datasets

3.1 Site descriptions

We compiled long-term HTDMA datasets from eight sites spanning urban, continental, mountainous, coastal urban, and marine environments. Five datasets were obtained from the U.S. Department of Energy Atmospheric Radiation Measurement (DOE ARM) program (Uin et al., 2012), and three were drwan from the literature (Xu, 2021; Ray et al., 2023; Fan et al., 2020).

https://doi.org/10.5194/egusphere-2026-4216
Preprint. Discussion started: 28 July 2026

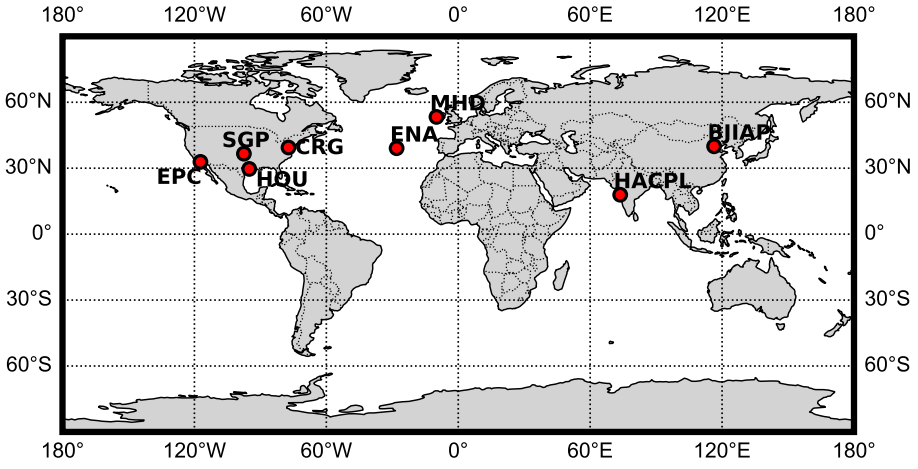

Figure 1. Sites with HTDMA measurements used in this study.

Together, these sites sample aerosol population influenced by urban emissions, continental background conditions, coastal and marine air masses, and high-altitude transport.

Urban sites include Baltimore, MD (CRG) and the Beijing Institute of Atmospheric Physics, China (BJIAP), both influenced by persistent anthropogenic emissions. The continental rural site at Lamont, OK (SGP) represents a region influenced by agricultural activity, biomass burning, and long-range transport. The High Altitude Cloud Physics Laboratory, India (HACPL) represents a mountainous environment with strong free-tropospheric influence. Coastal urban sites include La Jolla, CA (EPC) and Houston, TX (HOU), where urban emissions interact with nearby marine air masses. Mace Head Research Station, Ireland (MHD) represents a coastal site frequently influenced by alternating marine and continental air masses, while the Eastern North Atlantic site (ENA) represents a remote marine environment dominated by marine boundary layer conditions.

Because the available records differ in duration, seasonal coverage, and sampled particle sizes, the resulting climatology is intended to characterize broad cross-site and seasonal patterns rather than provide a fully harmonized trend analysis across all sites. The geographical distribution of all sites is shown in Figure 1, and measurement periods and available particle sizes for each site are summarized in Table 1.

3.2 Data processing

Across all sites, data were processed into a common κ-PDF framework for retrieval of χ, while preserving site-specific particle size grids and data availability. For the five ARM sites, κ values and particle number concentrations were extracted directly from the processed HTDMA data stream at each target diameter. For the BJIAP dataset, hygroscopic growth factors were first converted to κ using κ-Köhler theory at the measured relative humidity of 90%, with season-appropriate temperatures applied. For MHD and HACPL, κ-PDFs were constructed directly from the κ distributions provided in the respective datasets. For continental and coastal sites, κ-PDFs were constructed over the range $0 \leq \kappa \leq 0.65$, whereas for marine-influenced sites (ENA

https://doi.org/10.5194/egusphere-2026-4216
Preprint. Discussion started: 28 July 2026

Table 1. Summary of HTDMA measurement sites used in this study.

Site	Abbrev.	Type	Period	Source
Baltimore, MD, USA[a]	CRG	Urban	Mar 2025 – Nov 2025	ARM
Graciosa Island, Azores[a]	ENA	Marine	Aug 2021 – May 2023	ARM
La Jolla, CA, USA[a]	EPC	Coastal urban	Feb 2023 – Feb 2024	ARM
Mahabaleshwar, India[b]	HACPL	Mountainous	May 2019 – May 2020	Ray et al. (2023)
Houston, TX, USA[a]	HOU	Coastal urban	Oct 2021 – Sep 2022	ARM
Mace Head, Ireland[c]	MHD	Coastal	Nov 2010 – Mar 2014	Xu (2021)
Beijing, China[d]	BJIAP	Urban	Nov 2016; May–Jun 2017	Fan et al. (2020)
Lamont, OK, USA[a]	SGP	Continental	Apr 2021 – Oct 2023	ARM

Measured particle diameters (nm):
[a]50, 100, 150, 200, 250
[b]32, 50, 75, 100, 110, 150, 210, 260
[c]35, 50, 75, 110, 165
[d]40, 80, 110, 150, 200

and MHD) the range was extended to $0 \leq \kappa \leq 1.5$, to reflect the presence of highly hygroscopic species. As a result, χ values at ENA and MHD are not directly comparable to those from continental sites because different end-member assumptions are used.

For the ENA site, we implemented additional quality control procedures to remove periods influenced by local pollution sources near the measurement facility, including emissions from the nearby village, airport operations, diesel generators, and other island-based activities. To ensure the analysis reflects representative marine conditions rather than local pollution, a 6-minute pollution flag was derived from the 1-minute local pollution flag in the ARM data stream to match the temporal resolution of the HTDMA measurement cycle. The 1-minute pollution flag is derived from a combination of wind direction, particle number concentration spikes, and tracer species that indicate fresh combustion emissions (Zhou et al., 2025). This quality control procedure removed approximately 35% of the HTDMA measurements at ENA, with the highest rejection rates occurring during periods with unfavorable wind directions from the island interior and daytime hours when local anthropogenic activity is most prevalent. The local pollution flag primarily identifies periods affected by local anthropogenic contamination and does not exclude marine aerosol produced by processes such as shoreline wave breaking.

3.3 Spatial and temporal variation of aerosol hygroscopicity

Before presenting retrieved χ, we first examine the underlying seasonal κ-PDFs at representative sites to illustrate how hygroscopicity variability differs across environments and particle sizes. Figure 2 shows the seasonal κ-PDFs for three representative sites spanning continental (SGP), coastal urban (HOU), and marine (ENA) environments. The shape and width of these distributions reflect the degree of particle-to-particle hygroscopicity variability within each aerosol population.

https://doi.org/10.5194/egusphere-2026-4216
Preprint. Discussion started: 28 July 2026

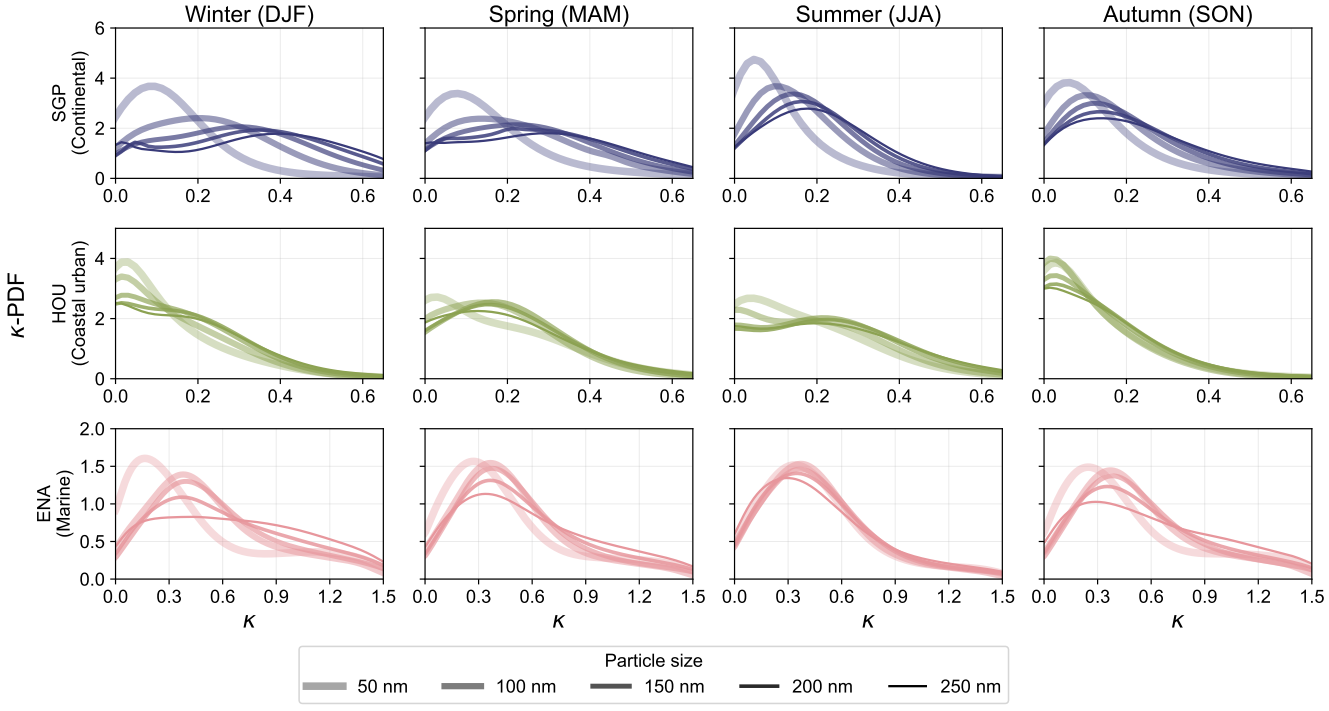

Figure 2. Seasonal κ-PDF for three representative sites: Southern Great Plains, OK (SGP, continental), Houston, TX (HOU, coastal urban), and Eastern North Atlantic, Azores (ENA, marine). Each panel shows the mean κ-PDF for a given season and particle size, averaged across all available days within the measurement period. Colors indicate site, while line opacity and thickness vary with particle diameter, with smaller particles shown as thicker and more opaque lines. The ENA dataset reflects measurements after removing locally polluted periods (see Section 3.2).

At the continental SGP site, the κ-PDFs exhibit pronounced seasonal variability and a strong size dependence. In winter and spring, the distributions are broad and multimodal. For 50-nm particles, a dominant peak appears at low κ values (0.05), while larger particles show an additional distinct mode at higher κ values extending toward 0.4–0.5. This pattern indicates the coexistence of multiple particle subpopulations with substantially different hygroscopicities, consistent with a diverse aerosol population influenced by agricultural burning, long-range transport of biomass burning aerosols, and enhanced nitrate formation under colder temperatures (Iziomon and Lohmann, 2003; Parworth et al., 2015b; Liu et al., 2021; Niedek et al., 2025b). In contrast, summer distributions are narrower and more unimodal across all sizes, suggesting a more chemically homogeneous aerosol population with reduced variability in hygroscopicity. The size dependence is most pronounced in winter and spring, where larger particles are significantly more hygroscopic than smaller ones.

At the coastal urban HOU site, the κ-PDFs show distinct seasonal variability, particularly for larger particles. Summer distributions are distinctly bimodal, whereas the other seasons are generally characterized by a single dominant mode. The autumn and winter distributions are notably narrow, indicating a more homogeneous aerosol population with limited particle-

https://doi.org/10.5194/egusphere-2026-4216
Preprint. Discussion started: 28 July 2026

to-particle variability in hygroscopicity. Across all seasons, small particles consistently show a dominant low-κ contribution, reflecting the persistent influence of fresh primary emissions from the Houston metropolitan area (Farley et al., 2024).

At the remote marine ENA site, the κ-PDFs extend to $\kappa = 1.5$ and are characterized by a peak centered around $\kappa \approx 0.3$, along with broad distribution for larger particles across all seasons, reflecting the wide hygroscopicity spectrum typical of marine aerosol populations. The 50-nm particles consistently show a distinct low-κ peak that is most pronounced in winter. Seasonal variability at ENA is moderate, with spring and autumn showing similar distributions across particle sizes. The influence of local pollution on the κ-PDFs is most evident in winter and autumn (Figure S1 in the Supplement), where the unfiltered distributions show a distinct low-κ peak compared to the filtered distributions.

The κ-PDFs for the remaining five sites (CRG, EPC, HACPL, BJIAP, and MHD) are shown in the Supplement (Figure S2). The urban CRG and coastal urban EPC show similar features to HOU, with a dominant low-κ contribution for small particles and broader distributions for larger particles across all seasons. The mountainous HACPL site displays notably narrow and unimodal distributions centered around $\kappa \approx 0.15$–0.20 across all sizes and seasons, indicating much less particle-to-particle hygroscopicity variability at this high-altitude environment. At the urban BJIAP site, the distributions are broader and bimodal, with winter distributions resemble the patterns observed at SGP. The coastal MHD site stands out from the other sites with distinctly multimodal distributions extending to $\kappa = 1.5$. The distinct peaks at around $\kappa \approx 0.3$ and $\kappa \approx 0.9$ indicate the coexistence of particles populations associated with alternating marine and continental air masses (Xu et al., 2020, 2021).

4 Aerosol mixing state climatology

4.1 Aerosol mixing state retrieval

Figure 3 shows the seasonal variablity of estimated χ across all sites and particle sizes. Across most sites, χ typically falls between 50% and 100%, indicating that ambient aerosol populations are often closer to the internally mixed than the externally mixed limit. At the same time, systematic differences in the median, spread, and seasonal variability of χ are evident across environments and particle sizes. This is consistent with previous observations of predominantly internally mixed aerosol populations derived from both field measurements and particle-resolved model simulations (Yuan and Zhao, 2023; Zhao et al., 2021b; Xue et al., 2024). Nevertheless, differences in the median, spread, and seasonal variability of χ are evident across sites.

The mountainous HACPL site exhibits consistently high χ values across all seasons and particle sizes. Winter and spring show particularly narrow interquartile ranges (IQR), indicating limited day-to-day variability in mixing state. In contrast, summer and autumn show wider spreads with more low-χ outliers, possibly reflecting the influence of the monsoon season introducing more diverse aerosol sources (Mukherjee et al., 2018). Overall, the consistently high χ values at HACPL suggest relatively well-mixed aerosol populations, with less influence from freshly emitted and compositionally distinct particle classes than at several other sites.

At the continental SGP site, χ values are generally high but show greater seasonal and size-dependent variability compared to HACPL. Large particles (> 150 nm) exhibit broader χ distributions in winter and spring compared to summer and autumn, while smaller particles show less seasonal variation. This size-dependent pattern is consistent with the bimodal κ-PDFs ob-

https://doi.org/10.5194/egusphere-2026-4216
Preprint. Discussion started: 28 July 2026

served at SGP in winter and spring, in contrast to the unimodal distributions observed in summer. The urban and coastal urban sites CRG, HOU, and EPC show broadly similar χ values, with high medians and relatively narrow spreads across all available seasons. These sites are characterized by persistent anthropogenic emission influences, and thus aerosol populations remain relatively internally mixed throughout the year. At the urban BJIAP site, χ shows a clear seasonal contrast between winter and summer. Winter exhibits lower median χ compare to summer across all sizes. In addition, smaller particles showing higher χ than larger particles. Compared to the other urban and coastal urban sites (CRG, HOU, and EPC), BJIAP exhibits broader spreads across all particle sizes and seasons, indicating greater day-to-day variability in aerosol mixing state, consistent with the diverse emission sources and rapid atmospheric processing characteristics of urban Beijing (Chen et al., 2020; Liu et al., 2025a).

At the ENA marine site, χ exhibits a clear size-dependent pattern along with greater variability than at the continental sites. Overall, ENA shows a wider spread in χ across all particle sizes and seasons, reflecting the diverse aerosol population at this location where clean marine air masses, long-range transported continental aerosols, and marine particles from both regional transport and local shoreline wave breaking coexist (Wang et al., 2021a; Zhou et al., 2025). Particles in the 100–200 nm range exhibit higher median χ values and narrower IQR compared to smaller and larger particles, indicating a more internally mixed aerosol population in the accumulation mode. This pattern is consistent with the strong influence of cloud processing in remote marine environments, where repeated cloud activation, aqueous-phase production, and subsequent evaporation tend to promote internal mixing. The bimodal aeorsol size distribution frequently observed at ENA further indicates the importance of cloud processing in this environment (Gong et al., 2023; Wang et al., 2021b). In contrast, the lower χ and wider spread observed for 50-nm particles likely reflects the coexistence of freshly produced marine particles and aged continental aerosols. The lower χ values observed at 250 nm may reflect increasing contributions from primary sea spray aerosol in addition to cloud-processed accumulation-mode particles, resulting in a compositionally diverse aerosol population.

The coastal MHD site exhibits the widest spread in χ of all sites, particularly for smaller particles in winter. A clear size-dependent pattern is evident across all seasons, with median χ increasing and spread decreasing with particle size. This consistent trend suggests that larger particles at MHD are more internally mixed, while smaller particles are subject to greater variability driven by the frequent alternation between clean marine and polluted continental air masses at this site (Xu et al., 2020, 2021). The pronounced high-κ modes observed in the winter κ-PDFs (Figure S2) further suggest episodic contributions from highly hygroscopic marine aerosol, potentially including sea-salt particles generated by coastal wave breaking (O'Dowd et al., 2014).

Across most sites, a modest size dependence in χ is evident, with larger particles generally showing higher median χ and narrower spreads compared to smaller particles, consistent with greater atmospheric aging of accumulation mode particles. Notable exceptions occur at the urban BJIAP site, where larger particles exhibit lower χ during winter, and the marine ENA site, where χ decreases for the largest particles. These patterns likely reflect the influence of distinct source populations, including externally mixed sea-salt aerosol at ENA and chemically diverse anthropogenic aerosol at BJIAP. A similar influence is evident at EPC during winter, when accumulation-mode particles exhibit lower χ than in other seasons due to stronger continental influence. This size-dependence of χ has direct implications for CCN predictions. Internal mixing assumptions are generally

https://doi.org/10.5194/egusphere-2026-4216
Preprint. Discussion started: 28 July 2026

more appropriate for larger accumulation-mode particles, which typically activate as CCN regardless of moderate variations in composition. In contrast, CCN activation of smaller Aitken-mode particles is more sensitive to particle hygrosopicity and mixing state, such that internal mixing assumptions may introduce systematic biases in predicted CCN concentrations (Gasparini et al., 2006; Patel and Jiang, 2021).

https://doi.org/10.5194/egusphere-2026-4216
Preprint. Discussion started: 28 July 2026

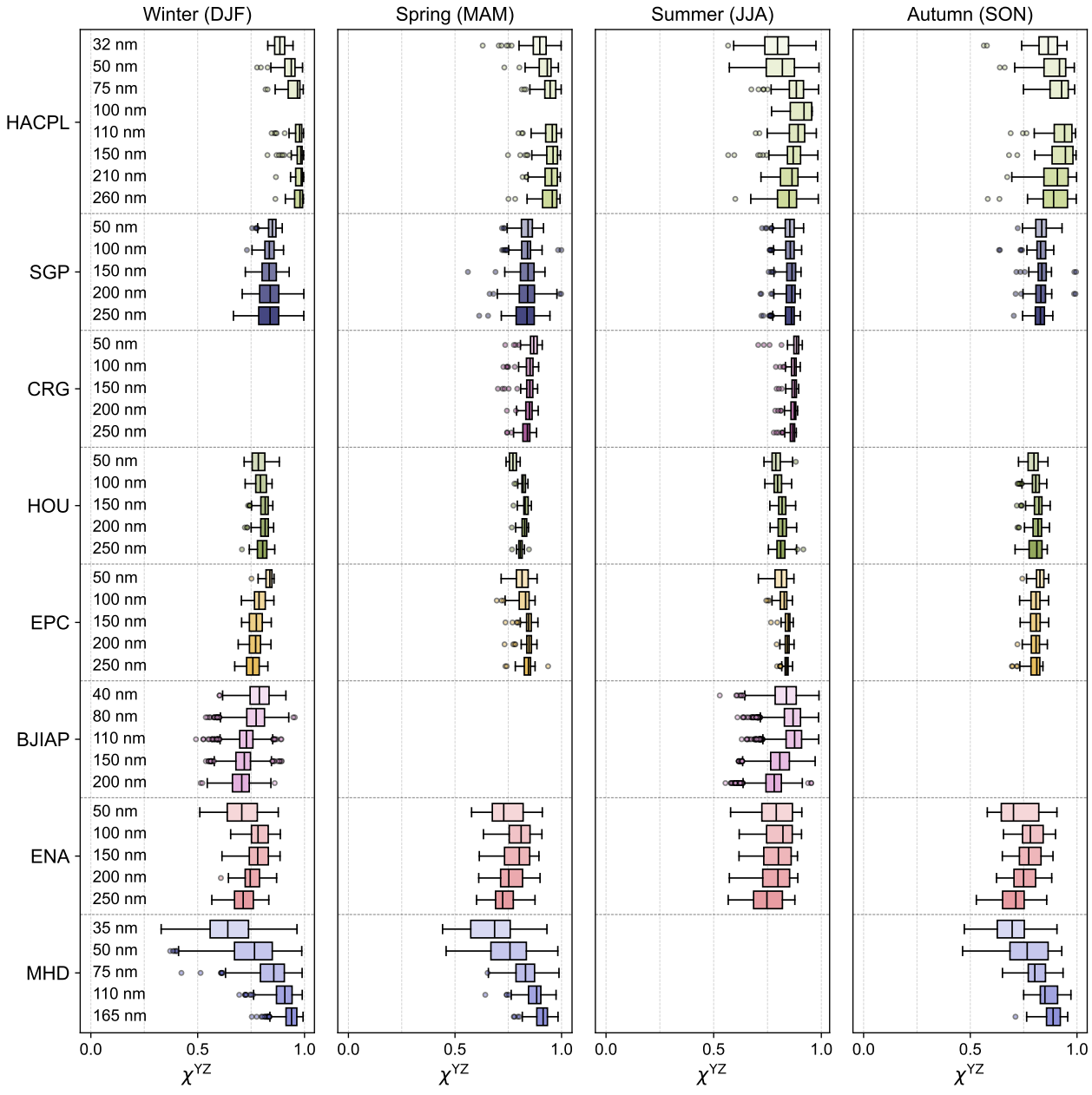

Figure 3. Seasonal variability of the aerosol mixing state index χ estimated from HTDMA measurements at eight sites. Each column represents a season (DJF: Winter; MAM: Spring; JJA: Summer; SON: Autumn). Colors represent individual sites and boxplots are arranged vertically by particle size, with smaller sizes at the top and larger sizes toward the bottom. In each boxplot, the left, central, and right edges correspond to the 25^{th} (q_1), 50^{th} (median), and 75^{th}(q_3) percentiles, respectively, while the whiskers extend to 1.5× the interquartile range ($IQR = q_3 - q_1$). Points beyond the whiskers indicate outliers.

https://doi.org/10.5194/egusphere-2026-4216
Preprint. Discussion started: 28 July 2026

4.2 Aerosol mixing state diagnostic analytics

To interpret whether changes in χ arise primarily from shifts in per-particle diversity, bulk population diversity, or both, we next examine the retrieval in D_α-D_γ space. Figure 4 examines the seasonal variability of χ through diversity metrics D_α and D_γ for three representative sites, with results for all eight sites provided in the Supplement (Figure S3 and S4) showing broadly similar size-dependent behavior. Each point in the D_α-D_γ diagram represents an aerosol population, where the position relative to the χ isolines characterizes its mixing state. Populations near the $\chi = 100\%$ line are nearly fully internally mixed, while populations located near lower χ lines reflect greater particle-to-particle compositional heterogeneity.

Across all sites and particle sizes, the D_α-D_γ diagram reveals several recurring patterns. Accumulation mode particles consistently show tighter clustering and shift toward larger values compared to Aitken mode particles. The reduced interannual and seasonal variability in the accumulation mode, together with the elevated diversity metrics, suggests that large particles are subject to more consistent atmospheric aging processes that progressively enrich their chemical composition (Kleinman et al., 2008; Jimenez et al., 2009; Ng et al., 2010; Peng et al., 2016; Liu et al., 2021). In contrast, Aitken mode particles show greater sensitivity to variability in emission sources.

At the continental SGP site, both Aitken (50nm) mode and accumulation (250 nm) mode particles show points distributed along a single χ isoline between 75% and 100%, indicating that the degree of internal mixing remains stable across seasons and years despite substantial variability in D_α and D_γ. The proportional covariation of D_α and D_γ along the χ isoline implies that the drivers of aerosol chemical complexity at SGP alter the overall richness of the population without preferentially enriching individual particles relative to the bulk. Winter and spring consistently show higher D_α and D_γ compared to summer, reflecting greater diversity in the relative abundance of LH and MH components among particles during the cooler seasons. This is consistent with enhanced nitrate formation under lower temperatures (Wang et al., 2023; Niedek et al., 2025a), increased contributions from biomass burning and agricultural activities in spring (Parworth et al., 2015a), and long-range transport from the southeast (Hu et al., 2025). The dispersion among same-colored points reflects year-to-year variability in D_α and D_γ within each season, which is more pronounced for 50-nm particles than for 250-nm particles.

At the coastal urban EPC site, Aitken mode particles exhibit the most pronounced seasonal variability in D_α and D_γ across all sites, yet the aerosol population remains at a consistent degree of internal mixing as both metrics covary proportionally. Aerosol diversities are lowest in winter, potentially due to the stronger continental air mass transport from the Los Angeles Basin, which brings fresher aerosols that remain externally mixed to the site, in contrast to spring and summer when marine and aged continental aerosol mix at the site (Guazzotti et al., 2001; Han et al., 2025). Under these conditions, accumulation mode particles in winter are also more externally mixed ($\chi \approx 75\%$) than in other seasons, possibly due to reduced photochemical activity and shorter atmospheric residence times.

The mountainous HACPL site exhibits a distinct seasonal pattern compared to other sites, with winter showing higher χ than summer for both Aitken and accumulation mode particles. The IQR is larger in winter for Aitken mode particles and in summer for accumulation mode particles, indicating greater day-to-day variability in these aerosol populations. For Aitken mode particles, the greater winter spread may reflect occasional fresh emissions. In contrast, summer conditions are influenced

https://doi.org/10.5194/egusphere-2026-4216
Preprint. Discussion started: 28 July 2026

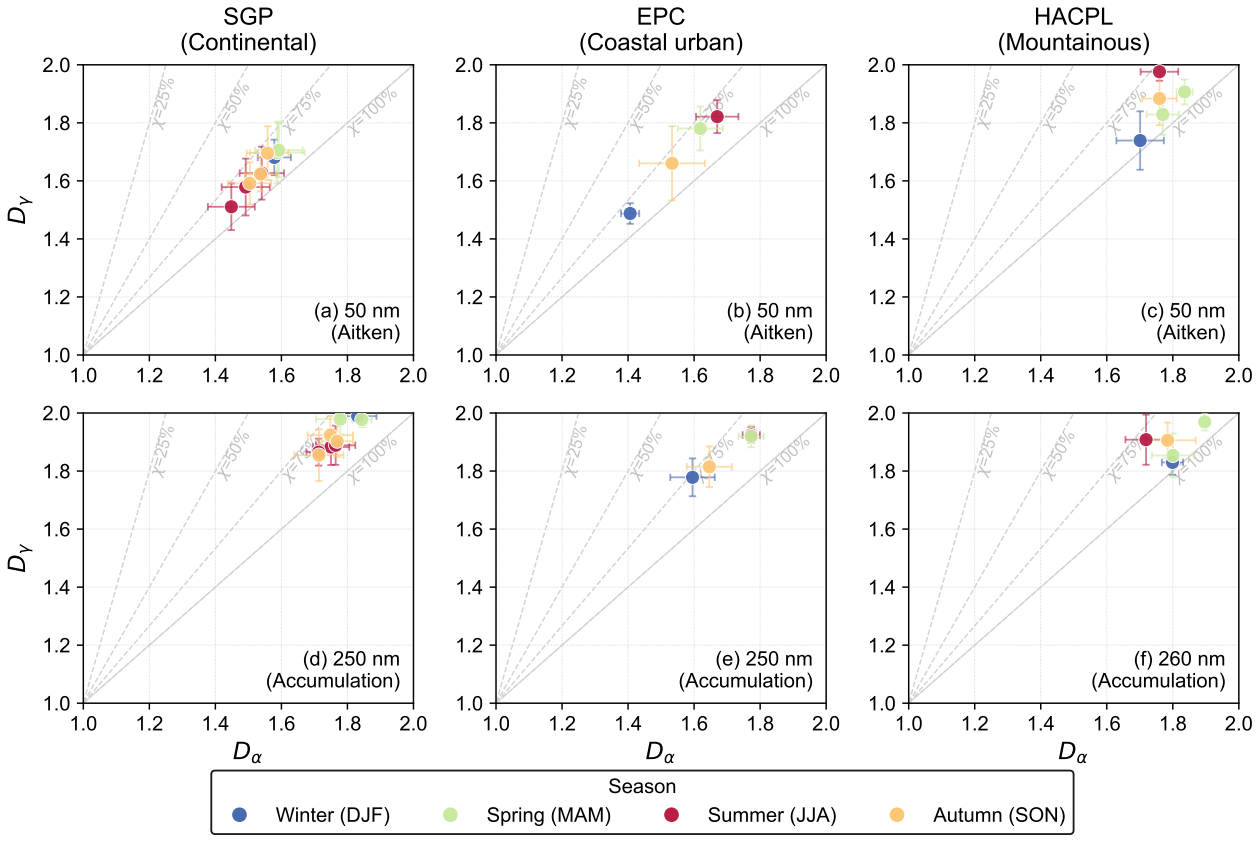

Figure 4. Seasonal mean per-particle diversity (D_α) and bulk population diversity (D_γ) for three representative sites: Southern Great Plain, OK (SGP, continental), La Jolla, CA (EPC, coastal urban), and High Altitude Cloud Physics Laboratory, India (HACPL, mountainous). Each point represents the seasonal mean and bars denote the interquartile range. Dashed lines represent mixing state index values of $\chi = 25\%$, 50%, 75%, and 100%. Panels (a)–(c) shows results for smaller (Aitken-mode) particles and panels (d)–(f) for larger (accumulation-mode) particles. Colors represent seasons as indicated in the legend.

by monsoon-driven circulation, which could introduce a more heterogeneous mixture of biogenic, marine, and anthropogenic aerosols from diverse source regions across the Indian subcontinent that have not fully aged.

Together, Figures 3 and 4 show that aerosol populations across these sites are often substantially internally mixed, but that the degree and variability of internal mixing depend systematically on particle size, season, and environment. Much of this variability can be understood as changes in the balance between per-particle diversity and bulk population diversity, rather than as a simple monotonic progression toward full internal mixing.

https://doi.org/10.5194/egusphere-2026-4216
Preprint. Discussion started: 28 July 2026

5 Conclusions

We present a climatology of aerosol mixing state index (χ) derived from hygroscopicity measurements at eight sites spanning diverse environments, including continental, urban, coastal urban, mountainous, marine, and coastal regimes. Building on previously evaluated retrieval framework ofYuan and Zhao (2023) and Liu et al. (2026), we examined seasonal, size-dependent, and site-type variability in χ and used the diversity metrics D_α and D_γ to investigate the processes underlying that variability.

Across all sites, the value of χ predominantly falls in the range of 50%–100%, indicating that ambient aerosol populations are generally more internally mixed than the externally mixed limit. At the same time, systematic deviations from full internal mixing remain evident and vary with particle size, season, and environment.

The degree of internal mixing varies systematically with particle size, with accumulation mode particles mostly showing higher χ and less seasonal variability than Aitken mode particles, reflecting the greater atmospheric aging of larger particles. This size dependence has direct implications for CCN activity predictions, as accumulation-mode particles generally activate over a wide range of compositions, whereas the CCN activity of Aitken-mode particles depends more strongly on particle composition and mixing state. Consequently, the internal mixing assumption commonly employed in atmospheric models becomes increasingly appropriate for larger particles but may introduce systematic biases for smaller particles. For marine-influenced sites, however, interpretation of χ requires additional care because highly hygroscopic species, such as sea salt, broaden the relevant hygroscopicity range and make the binary retrieval framework more approximate.

The D_α-D_γ diagram shows that the degree of internal mixing can remain relatively stable even when aerosol chemical complexity varies substantially. This occurs when average per-particle diversity (D_α) and bulk population diversity (D_γ) vary approximately proportionally, so that the overall richness of the aerosol population changes without substantially altering the relative homogeneity of individual particles. In contrast, seasonal changes in χ arise when D_α and D_γ do not covary proportionally. At the coastal urban EPC site, for example, winter accumulation-mode particles exhibit lower χ, consistent with stronger continental transport introducing chemically distinct particle types and increasing D_γ relative to D_α. At the mountainous HACPL site, monsoon-season transport from diverse source regions similarly appears to increase population-level diversity and reduce χ compared with the more aged, internally mixed aerosol that dominates during winter. In these cases, changes in chi are driven primarily by changes in bulk population diversity, suggesting that seasonal shifts in source contributions can play a larger role than progressive atmospheric aging in controlling aerosol mixing state.

The results provide observational constraints on aerosol mixing state across diverse environments and particle sizes, serving as benchmarks for evaluating mixing state representations in atmospheric models. The consistently high χ values observed across most sites and seasons suggest that the internal mixing assumption captures the dominant mixing state of ambient aerosol populations, particularly for accumulation mode particles. However, the systematic deviations from full internal mixing, especially for Aitken mode particles and at sites with diverse emission sources, highlight the need for more realistic aerosol representation in models used to simulate cloud activation. In contrast, aerosol optical properties are dominated by accumulation-mode particles, for which the internal mixing assumption is generally more appropriate, therefore, biases associated with this assumption are likely less significant for aerosol optical property calculation. In addition, the sensitivity of χ to

https://doi.org/10.5194/egusphere-2026-4216
Preprint. Discussion started: 28 July 2026

seasonal changes in aerosol sources and atmospheric processes suggests that long-term mixing-state observations could serve as valuable indicators of regional air quality evolution and the effectiveness of emission control strategies.

This work highlights several directions for future research. First, the eight sites examined here are confined to the Northern Hemisphere and do not include tropical or polar environments where aerosol mixing state may exhibit distinct characteristics. Expanding the measurement network to underrepresented regions would establish a more comprehensive global climatology of aerosol mixing state. Second, the temporal coverage across sites varies considerably, with some providing only limited seasonal sampling rather than continuous multi-year records. Longer and more continuous HTDMA measurement records would better characterize interannual variability and potential long-term trends in aerosol mixing state.

Data availability. The data and code used to reproduce the figures are available at https://databank.illinois.edu/datasets/IDB-8600813?code=TvVx5g01qmigDHr5dgUzQ5NPb6Z9unIh4Xu7dfjquNM.

https://doi.org/10.5194/egusphere-2026-4216
Preprint. Discussion started: 28 July 2026

Author contributions. YL contributed to the study design, conducted the data analysis, and wrote the manuscript. SZ contributed expertise on aerosol measurements at coastal and remote marine sites and provided guidance on the quality control of the ENA observations. JW contributed to the interpretation of the results and discussions of marine aerosol processes. NR supervised the study and provided scientific guidance throughout the project. All authors reviewed the manuscript, provided comments and revisions, and approved the final version.

Competing interests. The authors declare that they have no conflict of interest.

Acknowledgements. This work was supported by DOE ASR grant DE-SC0025197 and DE-SC0025873.

https://doi.org/10.5194/egusphere-2026-4216
Preprint. Discussion started: 28 July 2026

References

Adachi, K., Tobo, Y., Koike, M., Freitas, G., Zieger, P., and Krejci, R.: Composition and Mixing State of Arctic Aerosol and Cloud Residual Particles from Long-Term Single-Particle Observations at Zeppelin Observatory, Svalbard, Atmospheric Chemistry and Physics, 22, 14 421–14 439, https://doi.org/10.5194/acp-22-14421-2022, 2022.

Baustian, K. J., Cziczo, D. J., Wise, M. E., Pratt, K. A., Kulkarni, G., Hallar, A. G., and Tolbert, M. A.: Importance of Aerosol Composition, Mixing State, and Morphology for Heterogeneous Ice Nucleation: A Combined Field and Laboratory Approach, Journal of Geophysical Research: Atmospheres, 117, https://doi.org/10.1029/2011JD016784, 2012.

Bondy, A. L., Bonanno, D., Moffet, R. C., Wang, B., Laskin, A., and Ault, A. P.: The Diverse Chemical Mixing State of Aerosol Particles in the Southeastern United States, Atmospheric Chemistry and Physics, 18, 12 595–12 612, https://doi.org/10.5194/acp-18-12595-2018, 2018.

Chen, Y., Cai, J., Wang, Z., Peng, C., Yao, X., Tian, M., Han, Y., Shi, G., Shi, Z., Liu, Y., Yang, X., Zheng, M., Zhu, T., He, K., Zhang, Q., and Yang, F.: Simultaneous Measurements of Urban and Rural Particles in Beijing – Part 1: Chemical Composition and Mixing State, Atmospheric Chemistry and Physics, 20, 9231–9247, https://doi.org/10.5194/acp-20-9231-2020, 2020.

Chin, M., Ginoux, P., Kinne, S., Torres, O., Holben, B. N., Duncan, B. N., Martin, R. V., Logan, J. A., Higurashi, A., and Nakajima, T.: Tropospheric Aerosol Optical Thickness from the GOCART Model and Comparisons with Satellite and Sun Photometer Measurements, Journal of the Atmospheric Sciences, 59, 461–483, https://doi.org/10.1175/1520-0469(2002)059<0461:TAOTFT>2.0.CO;2, 2002.

Cubison, M. J., Ervens, B., Feingold, G., Docherty, K. S., Ulbrich, I. M., Shields, L., Prather, K., Hering, S., and Jimenez, J. L.: The Influence of Chemical Composition and Mixing State of Los Angeles Urban Aerosol on CCN Number and Cloud Properties, Atmospheric Chemistry and Physics, 8, 5649–5667, https://doi.org/10.5194/acp-8-5649-2008, 2008.

Ebert, M., Weinbruch, S., Hoffmann, P., and Ortner, H. M.: The Chemical Composition and Complex Refractive Index of Rural and Urban Influenced Aerosols Determined by Individual Particle Analysis, Atmospheric Environment, 38, 6531–6545, https://doi.org/10.1016/j.atmosenv.2004.08.048, 2004.

Fan, X., Liu, J., Zhang, F., Chen, L., Collins, D., Xu, W., Jin, X., Ren, J., Wang, Y., Wu, H., Li, S., Sun, Y., and Li, Z.: Contrasting Size-Resolved Hygroscopicity of Fine Particles Derived by HTDMA and HR-ToF-AMS Measurements between Summer and Winter in Beijing: The Impacts of Aerosol Aging and Local Emissions, Atmospheric Chemistry and Physics, 20, 915–929, https://doi.org/10.5194/acp-20-915-2020, 2020.

Farley, R. N., Lee, J. E., Rivellini, L.-H., Lee, A. K. Y., Dal Porto, R., Cappa, C. D., Gorkowski, K., Shawon, A. S. M., Benedict, K. B., Aiken, A. C., Dubey, M. K., and Zhang, Q.: Chemical Properties and Single-Particle Mixing State of Soot Aerosol in Houston during the TRACER Campaign, Atmospheric Chemistry and Physics, 24, 3953–3971, https://doi.org/10.5194/acp-24-3953-2024, 2024.

Fraund, M., Pham, D. Q., Bonanno, D., Harder, T. H., Wang, B., Brito, J., De Sá, S. S., Carbone, S., China, S., Artaxo, P., Martin, S. T., Pöhlker, C., Andreae, M. O., Laskin, A., Gilles, M. K., and Moffet, R. C.: Elemental Mixing State of Aerosol Particles Collected in Central Amazonia during GoAmazon2014/15, Atmosphere, 8, 173, https://doi.org/10.3390/atmos8090173, 2017.

Gasparini, R., Li, R., Collins, D. R., Ferrare, R. A., and Brackett, V. G.: Application of Aerosol Hygroscopicity Measured at the Atmospheric Radiation Measurement Program's Southern Great Plains Site to Examine Composition and Evolution, Journal of Geophysical Research: Atmospheres, 111, https://doi.org/10.1029/2004JD005448, 2006.

https://doi.org/10.5194/egusphere-2026-4216
Preprint. Discussion started: 28 July 2026

Gong, X., Wang, Y., Xie, H., Zhang, J., Lu, Z., Wood, R., Stratmann, F., Wex, H., Liu, X., and Wang, J.: Maximum Supersaturation in the Marine Boundary Layer Clouds Over the North Atlantic, AGU Advances, 4, e2022AV000 855, https://doi.org/10.1029/2022AV000855, 2023.

Guazzotti, S. A., Whiteaker, J. R., Suess, D., Coffee, K. R., and Prather, K. A.: Real-Time Measurements of the Chemical Composition of Size-Resolved Particles during a Santa Ana Wind Episode, California USA, Atmospheric Environment, 35, 3229–3240, https://doi.org/10.1016/S1352-2310(01)00140-6, 2001.

Han, S., Williams, A. S., Russell, L. M., Berta, V. Z., Dedrick, J. L., Pelayo, C., Maneenoi, N., Osawa, A., Silber, I., Zhang, D., Zawadowicz, M. A., and Sedlacek, A. J. I.: Nearby Sites Show Similar Upwind Sources and Differing Semivolatile Concentrations in Coastal Aerosol Particles, ACS ES&T Air, 2, 2824–2837, https://doi.org/10.1021/acsestair.5c00191, 2025.

Hu, R., Li, Z., and Su, T.: Investigating Aerosol Hygroscopicity in the Subcloud Transition Zone and at the Surface in the Southern Great Plains, Journal of Geophysical Research: Atmospheres, 130, e2024JD041 925, https://doi.org/10.1029/2024JD041925, 2025.

Iziomon, M. G. and Lohmann, U.: Characteristics and Direct Radiative Effect of Mid-Latitude Continental Aerosols: The ARM Case, Atmospheric Chemistry and Physics, 3, 1903–1917, https://doi.org/10.5194/acp-3-1903-2003, 2003.

Jimenez, J. L., Canagaratna, M. R., Donahue, N. M., Prevot, A. S. H., Zhang, Q., Kroll, J. H., DeCarlo, P. F., Allan, J. D., Coe, H., Ng, N. L., Aiken, A. C., Docherty, K. S., Ulbrich, I. M., Grieshop, A. P., Robinson, A. L., Duplissy, J., Smith, J. D., Wilson, K. R., Lanz, V. A., Hueglin, C., Sun, Y. L., Tian, J., Laaksonen, A., Raatikainen, T., Rautiainen, J., Vaattovaara, P., Ehn, M., Kulmala, M., Tomlinson, J. M., Collins, D. R., Cubison, M. J., E., Dunlea, J., Huffman, J. A., Onasch, T. B., Alfarra, M. R., Williams, P. I., Bower, K., Kondo, Y., Schneider, J., Drewnick, F., Borrmann, S., Weimer, S., Demerjian, K., Salcedo, D., Cottrell, L., Griffin, R., Takami, A., Miyoshi, T., Hatakeyama, S., Shimono, A., Sun, J. Y., Zhang, Y. M., Dzepina, K., Kimmel, J. R., Sueper, D., Jayne, J. T., Herndon, S. C., Trimborn, A. M., Williams, L. R., Wood, E. C., Middlebrook, A. M., Kolb, C. E., Baltensperger, U., and Worsnop, D. R.: Evolution of Organic Aerosols in the Atmosphere, Science, 326, 1525–1529, https://doi.org/10.1126/science.1180353, 2009.

Kleeman, M. J. and Cass, G. R.: A 3D Eulerian Source-Oriented Model for an Externally Mixed Aerosol, Environmental Science & Technology, 35, 4834–4848, https://doi.org/10.1021/es010886m, 2001.

Kleinman, L. I., Springston, S. R., Daum, P. H., Lee, Y.-N., Nunnermacker, L. J., Senum, G. I., Wang, J., Weinstein-Lloyd, J., Alexander, M. L., Hubbe, J., Ortega, J., Canagaratna, M. R., and Jayne, J.: The Time Evolution of Aerosol Composition over the Mexico City Plateau, Atmospheric Chemistry and Physics, 8, 1559–1575, https://doi.org/10.5194/acp-8-1559-2008, 2008.

Laskin, A., Laskin, J., and Nizkorodov, S. A.: Mass Spectrometric Approaches for Chemical Characterisation of Atmospheric Aerosols: Critical Review of the Most Recent Advances, Environmental Chemistry, 9, 163–189, https://doi.org/10.1071/EN12052, 2012.

Lata, N. N., Zhang, B., Schum, S., Mazzoleni, L., Brimberry, R., Marcus, M. A., Cantrell, W. H., Fialho, P., Mazzoleni, C., and China, S.: Aerosol Composition, Mixing State, and Phase State of Free Tropospheric Particles and Their Role in Ice Cloud Formation, ACS Earth and Space Chemistry, 5, 3499–3510, https://doi.org/10.1021/acsearthspacechem.1c00315, 2021.

Leck, C. and Svensson, E.: Importance of Aerosol Composition and Mixing State for Cloud Droplet Activation over the Arctic Pack Ice in Summer, Atmospheric Chemistry and Physics, 15, 2545–2568, https://doi.org/10.5194/acp-15-2545-2015, 2015.

Liu, J., Alexander, L., Fast, J. D., Lindenmaier, R., and Shilling, J. E.: Aerosol Characteristics at the Southern Great Plains Site during the HI-SCALE Campaign, Atmospheric Chemistry and Physics, 21, 5101–5116, https://doi.org/10.5194/acp-21-5101-2021, 2021.

Liu, J., Zhang, F., Ren, J., Chen, L., Zhang, A., Wang, Z., Zou, S., Xu, H., and Yue, X.: The Evolution of Aerosol Mixing State Derived from a Field Campaign in Beijing: Implications for Particle Aging Timescales in Urban Atmospheres, Atmospheric Chemistry and Physics, 25, 5075–5086, https://doi.org/10.5194/acp-25-5075-2025, 2025a.

https://doi.org/10.5194/egusphere-2026-4216
Preprint. Discussion started: 28 July 2026

Liu, Y., Yao, Y., Curtis, J. H., West, M., and Riemer, N.: The Impacts of Aerosol Mixing State on Heterogeneous N2O5 Hydrolysis, Aerosol Science and Technology, 59, 402–423, https://doi.org/10.1080/02786826.2024.2443587, 2025b.

Liu, Y., Wang, J., and Riemer, N.: From κ To χ: Evaluating Hygroscopicity-Based Mixing State Estimates with a Particle-Resolved Model, EGUsphere, pp. 1–19, https://doi.org/10.5194/egusphere-2026-1724, 2026.

Moffet, R. C., Henn, T. R., Tivanski, A. V., Hopkins, R. J., Desyaterik, Y., Kilcoyne, A. L. D., Tyliszczak, T., Fast, J., Barnard, J., Shutthanandan, V., Cliff, S. S., Perry, K. D., Laskin, A., and Gilles, M. K.: Microscopic Characterization of Carbonaceous Aerosol Particle Aging in the Outflow from Mexico City, Atmospheric Chemistry and Physics, 10, 961–976, https://doi.org/10.5194/acp-10-961-2010, 2010.

Mukherjee, S., Singla, V., Pandithurai, G., Safai, P. D., Meena, G. S., Dani, K. K., and Anil Kumar, V.: Seasonal Variability in Chemical Composition and Source Apportionment of Sub-Micron Aerosol over a High Altitude Site in Western Ghats, India, Atmospheric Environment, 180, 79–92, https://doi.org/10.1016/j.atmosenv.2018.02.048, 2018.

Ng, N. L., Canagaratna, M. R., Zhang, Q., Jimenez, J. L., Tian, J., Ulbrich, I. M., Kroll, J. H., Docherty, K. S., Chhabra, P. S., Bahreini, R., Murphy, S. M., Seinfeld, J. H., Hildebrandt, L., Donahue, N. M., DeCarlo, P. F., Lanz, V. A., Prévôt, A. S. H., Dinar, E., Rudich, Y., and Worsnop, D. R.: Organic Aerosol Components Observed in Northern Hemispheric Datasets from Aerosol Mass Spectrometry, Atmospheric Chemistry and Physics, 10, 4625–4641, https://doi.org/10.5194/acp-10-4625-2010, 2010.

Niedek, C., Mei, F., Jiang, W., Trousdell, J., Zawadowicz, M., Schmid, B., and Zhang, Q.: Advancing Aerosol Chemical Characterization and Vertical Profiling over the Southern Great Plains Using Uncrewed Aerial Sampling and Offline Aerosol Mass Spectrometry, ACS ES&T Air, 2, 2131–2146, https://doi.org/10.1021/acsestair.5c00128, 2025a.

Niedek, C., Mei, F., Jiang, W., Trousdell, J., Zawadowicz, M., Schmid, B., and Zhang, Q.: Advancing Aerosol Chemical Characterization and Vertical Profiling over the Southern Great Plains Using Uncrewed Aerial Sampling and Offline Aerosol Mass Spectrometry, ACS ES&T Air, 2, 2131–2146, https://doi.org/10.1021/acsestair.5c00128, 2025b.

O'Dowd, C., Ceburnis, D., Ovadnevaite, J., Vaishya, A., Rinaldi, M., and Facchini, M. C.: Do Anthropogenic, Continental or Coastal Aerosol Sources Impact on a Marine Aerosol Signature at Mace Head?, Atmospheric Chemistry and Physics, 14, 10 687–10 704, https://doi.org/10.5194/acp-14-10687-2014, 2014.

Parworth, C., Fast, J., Mei, F., Shippert, T., Sivaraman, C., Tilp, A., Watson, T., and Zhang, Q.: Long-Term Measurements of Submicrometer Aerosol Chemistry at the Southern Great Plains (SGP) Using an Aerosol Chemical Speciation Monitor (ACSM), Atmospheric Environment, 106, 43–55, https://doi.org/10.1016/j.atmosenv.2015.01.060, 2015a.

Parworth, C., Fast, J., Mei, F., Shippert, T., Sivaraman, C., Tilp, A., Watson, T., and Zhang, Q.: Long-Term Measurements of Submicrometer Aerosol Chemistry at the Southern Great Plains (SGP) Using an Aerosol Chemical Speciation Monitor (ACSM), Atmospheric Environment, 106, 43–55, https://doi.org/10.1016/j.atmosenv.2015.01.060, 2015b.

Patel, P. N. and Jiang, J. H.: Cloud Condensation Nuclei Characteristics at the Southern Great Plains Site: Role of Particle Size Distribution and Aerosol Hygroscopicity, Environmental Research Communications, 3, 075 002, https://doi.org/10.1088/2515-7620/ac0e0b, 2021.

Peng, J., Hu, M., Guo, S., Du, Z., Zheng, J., Shang, D., Levy Zamora, M., Zeng, L., Shao, M., Wu, Y.-S., Zheng, J., Wang, Y., Glen, C. R., Collins, D. R., Molina, M. J., and Zhang, R.: Markedly Enhanced Absorption and Direct Radiative Forcing of Black Carbon under Polluted Urban Environments, Proceedings of the National Academy of Sciences, 113, 4266–4271, https://doi.org/10.1073/pnas.1602310113, 2016.

Ray, A., Pandithurai, G., Mukherjee, S., Kumar, V. A., Hazra, A., Patil, R. D., and Waghmare, V.: Seasonal Variability in Size-Resolved Hygroscopicity of Sub-Micron Aerosols over the Western Ghats, India: Closure and Parameterization, Science of The Total Environment, 869, 161 753, https://doi.org/10.1016/j.scitotenv.2023.161753, 2023.

https://doi.org/10.5194/egusphere-2026-4216
Preprint. Discussion started: 28 July 2026

Riemer, N. and West, M.: Quantifying Aerosol Mixing State with Entropy and Diversity Measures, Atmospheric Chemistry and Physics, 13, 11 423–11 439, https://doi.org/10.5194/acp-13-11423-2013, 2013.

Uin, J., Cromwell, E., Hayes, C., and Salwen, C.: Atmospheric Radiation Measurement (ARM) User Facility. Humidified Tandem Differential Mobility Analyzer (AOSHTDMA), updated daily. 2025-03-13 to 2025-11-30, ARM Mobile Facility (CRG), Baltimore, MD: Supplemental Facility 2 in rural setting (S2); 2021-08-17 to 2023-05-24, Eastern North Atlantic (ENA), Graciosa Island, Azores, Portugal (C1); 2023-02-15 to 2024-02-13, ARM Mobile Facility (EPC), La Jolla, CA: AMF1 (main site for EPCAPE on Scripps Pier) (M1); 2021-10-01 to 2022-09-30, ARM Mobile Facility (HOU), Houston, TX: AMF1 (main site for TRACER) (M1); 2021-04-27 to 2023-10-24, Southern Great Plains (SGP), Lamont, OK (Extended and Co-located with C1) (E13). Compiled by Uin, J., Cromwell, E., Hayes, C., and Salwen, C. Data set accessed 2025-08-06 at https://doi.org/10.5439/1776643, 2012.

Wang, J., Cubison, M. J., Aiken, A. C., Jimenez, J. L., and Collins, D. R.: The Importance of Aerosol Mixing State and Size-Resolved Composition on CCN Concentration and the Variation of the Importance with Atmospheric Aging of Aerosols, Atmospheric Chemistry and Physics, 10, 7267–7283, https://doi.org/10.5194/acp-10-7267-2010, 2010.

Wang, Y., Zheng, G., Jensen, M. P., Knopf, D. A., Laskin, A., Matthews, A. A., Mechem, D., Mei, F., Moffet, R., Sedlacek, A. J., Shilling, J. E., Springston, S., Sullivan, A., Tomlinson, J., Veghte, D., Weber, R., Wood, R., Zawadowicz, M. A., and Wang, J.: Vertical Profiles of Trace Gas and Aerosol Properties over the Eastern North Atlantic: Variations with Season and Synoptic Condition, Atmospheric Chemistry and Physics, 21, 11 079–11 098, https://doi.org/10.5194/acp-21-11079-2021, 2021a.

Wang, Y., Zheng, G., Jensen, M. P., Knopf, D. A., Laskin, A., Matthews, A. A., Mechem, D., Mei, F., Moffet, R., Sedlacek, A. J., Shilling, J. E., Springston, S., Sullivan, A., Tomlinson, J., Veghte, D., Weber, R., Wood, R., Zawadowicz, M. A., and Wang, J.: Vertical Profiles of Trace Gas and Aerosol Properties over the Eastern North Atlantic: Variations with Season and Synoptic Condition, Atmospheric Chemistry and Physics, 21, 11 079–11 098, https://doi.org/10.5194/acp-21-11079-2021, 2021b.

Wang, Y., Bagya Ramesh, C., Giangrande, S. E., Fast, J., Gong, X., Zhang, J., Tolga Odabasi, A., Oliveira, M. V. B., Matthews, A., Mei, F., Shilling, J. E., Tomlinson, J., Wang, D., and Wang, J.: Examining the Vertical Heterogeneity of Aerosols over the Southern Great Plains, Atmospheric Chemistry and Physics, 23, 15 671–15 691, https://doi.org/10.5194/acp-23-15671-2023, 2023.

Wu, J., Liu, J., Gunsch, M. J., Mirrielees, J. A., Moffett, C. E., Zhang, Q., Sheesley, R. J., and Pratt, K. A.: Quantifying the Diversity of an Atmospheric Aerosol Population in an Arctic Oil Field on a Single-Particle Level, Journal of Geophysical Research: Atmospheres, 129, e2024JD041 001, https://doi.org/10.1029/2024JD041001, 2024.

Xu, W.: Sea Spray Aerosol Number Size Distribution Study, https://doi.org/10.17632/gjdd5r4ywf.1, data set accessed 2025-08-20 at https://data.mendeley.com/datasets/gjdd5r4ywf/1, 2021.

Xu, W., Ovadnevaite, J., Fossum, K. N., Lin, C., Huang, R.-J., O'Dowd, C., and Ceburnis, D.: Aerosol Hygroscopicity and Its Link to Chemical Composition in the Coastal Atmosphere of Mace Head: Marine and Continental Air Masses, Atmospheric Chemistry and Physics, 20, 3777–3791, https://doi.org/10.5194/acp-20-3777-2020, 2020.

Xu, W., Ovadnevaite, J., Fossum, K. N., Lin, C., Huang, R.-J., O'Dowd, C., and Ceburnis, D.: Seasonal Trends of Aerosol Hygroscopicity and Mixing State in Clean Marine and Polluted Continental Air Masses Over the Northeast Atlantic, Journal of Geophysical Research: Atmospheres, 126, e2020JD033 851, https://doi.org/10.1029/2020JD033851, 2021.

Xue, J., Zhang, T., Park, K., Yan, J., Yoon, Y. J., Park, J., and Wang, B.: Diverse Sources and Aging Change the Mixing State and Ice Nucleation Properties of Aerosol Particles over the Western Pacific and Southern Ocean, Atmospheric Chemistry and Physics, 24, 7731–7754, https://doi.org/10.5194/acp-24-7731-2024, 2024.

https://doi.org/10.5194/egusphere-2026-4216
Preprint. Discussion started: 28 July 2026

Yao, Y., Curtis, J. H., Ching, J., Zheng, Z., and Riemer, N.: Quantifying the Effects of Mixing State on Aerosol Optical Properties, Atmospheric Chemistry and Physics, 22, 9265–9282, https://doi.org/10.5194/acp-22-9265-2022, 2022.

Yuan, L. and Zhao, C.: Quantifying Particle-to-Particle Heterogeneity in Aerosol Hygroscopicity, Atmospheric Chemistry and Physics, 23, 3195–3205, https://doi.org/10.5194/acp-23-3195-2023, 2023.

Zaveri, R. A., Shaw, W. J., Cziczo, D. J., Schmid, B., Ferrare, R. A., Alexander, M. L., Alexandrov, M., Alvarez, R. J., Arnott, W. P., Atkinson, D. B., Baidar, S., Banta, R. M., Barnard, J. C., Beranek, J., Berg, L. K., Brechtel, F., Brewer, W. A., Cahill, J. F., Cairns, B., Cappa, C. D., Chand, D., China, S., Comstock, J. M., Dubey, M. K., Easter, R. C., Erickson, M. H., Fast, J. D., Floerchinger, C., Flowers, B. A., Fortner, E., Gaffney, J. S., Gilles, M. K., Gorkowski, K., Gustafson, W. I., Gyawali, M., Hair, J., Hardesty, R. M., Harworth, J. W., Herndon, S., Hiranuma, N., Hostetler, C., Hubbe, J. M., Jayne, J. T., Jeong, H., Jobson, B. T., Kassianov, E. I., Kleinman, L. I., Kluzek, C., Knighton, B., Kolesar, K. R., Kuang, C., Kubátová, A., Langford, A. O., Laskin, A., Laulainen, N., Marchbanks, R. D., Mazzoleni, C., Mei, F., Moffet, R. C., Nelson, D., Obland, M. D., Oetjen, H., Onasch, T. B., Ortega, I., Ottaviani, M., Pekour, M., Prather, K. A., Radney, J. G., Rogers, R. R., Sandberg, S. P., Sedlacek, A., Senff, C. J., Senum, G., Setyan, A., Shilling, J. E., Shrivastava, M., Song, C., Springston, S. R., Subramanian, R., Suski, K., Tomlinson, J., Volkamer, R., Wallace, H. W., Wang, J., Weickmann, A. M., Worsnop, D. R., Yu, X.-Y., Zelenyuk, A., and Zhang, Q.: Overview of the 2010 Carbonaceous Aerosols and Radiative Effects Study (CARES), Atmospheric Chemistry and Physics, 12, 7647–7687, https://doi.org/10.5194/acp-12-7647-2012, 2012.

Zeng, L., Tan, T., Zhao, G., Du, Z., Hu, S., Shang, D., and Hu, M.: Overestimation of Black Carbon Light Absorption Due to Mixing State Heterogeneity, npj Climate and Atmospheric Science, 7, 2, https://doi.org/10.1038/s41612-023-00535-8, 2024.

Zhao, G., Tan, T., Zhu, Y., Hu, M., and Zhao, C.: Method to Quantify Black Carbon Aerosol Light Absorption Enhancement with a Mixing State Index, Atmospheric Chemistry and Physics, 21, 18 055–18 063, https://doi.org/10.5194/acp-21-18055-2021, 2021a.

Zhao, G., Tan, T., Zhu, Y., Hu, M., and Zhao, C.: Method to Quantify Black Carbon Aerosol Light Absorption Enhancement with a Mixing State Index, Atmospheric Chemistry and Physics, 21, 18 055–18 063, https://doi.org/10.5194/acp-21-18055-2021, 2021b.

Zheng, Z., West, M., Zhao, L., Ma, P.-L., Liu, X., and Riemer, N.: Quantifying the Structural Uncertainty of the Aerosol Mixing State Representation in a Modal Model, Atmospheric Chemistry and Physics, 21, 17 727–17 741, https://doi.org/10.5194/acp-21-17727-2021, 2021.

Zhou, S., Salter, M., Bertram, T., Brito Azevedo, E., Reis, F., and Wang, J.: Shoreline Wave Breaking Strongly Enhances the Coastal Sea Spray Aerosol Population: Climate and Air Quality Implications, Science Advances, 11, eadw0343, https://doi.org/10.1126/sciadv.adw0343, 2025.

Zhu, S., Sartelet, K., Zhang, Y., and Nenes, A.: Three-Dimensional Modeling of the Mixing State of Particles over Greater Paris, Journal of Geophysical Research: Atmospheres, 121, 5930–5947, https://doi.org/10.1002/2015JD024241, 2016.